Divergent roles of haptoglobin and hemopexin deficiency for disease progression of Shiga-toxin-induced hemolytic-uremic syndrome in mice

Divergent roles of haptoglobin and hemopexin deficiency for disease progression of Shiga-toxin-induced hemolytic-uremic syndrome in mice

Wiebke Pirschel, M. Sc., Antonio N. Mestekemper, B. A., Bianka Wissuwa, Ph.D., Nadine Krieg, Ph.D., Sarah Kröller, M. Sc., Christoph Daniel, Prof., Florian Gunzer, Prof., Emanuela Tolosano, Prof., Michael Bauer, Prof., Kerstin Amann, Prof., Stefan H. Heinemann, Prof., Sina M. Coldewey, Prof.

PII: S0085-2538(22)00016-3

DOI: https://doi.org/10.1016/j.kint.2021.12.024

Reference: KINT 2901

To appear in: *Kidney International*

Received Date: 23 February 2021

Revised Date: 5 December 2021

Accepted Date: 16 December 2021

Please cite this article as: Pirschel W, Mestekemper AN, Wissuwa B, Krieg N, Kröller S, Daniel C, Gunzer F, Tolosano E, Bauer M, Amann K, Heinemann SH, Coldewey SM, Divergent roles of haptoglobin and hemopexin deficiency for disease progression of Shiga-toxin-induced hemolytic-uremic syndrome in mice, *Kidney International* (2022), doi: https://doi.org/10.1016/j.kint.2021.12.024.

Divergent roles of haptoglobin and hemopexin deficiency for disease progression of Shiga-toxin-induced hemolytic-uremic syndrome in mice

kidney INTERNATIONAL

ISN INTERNATIONAL SOCIETY OF NEPHROLOGY

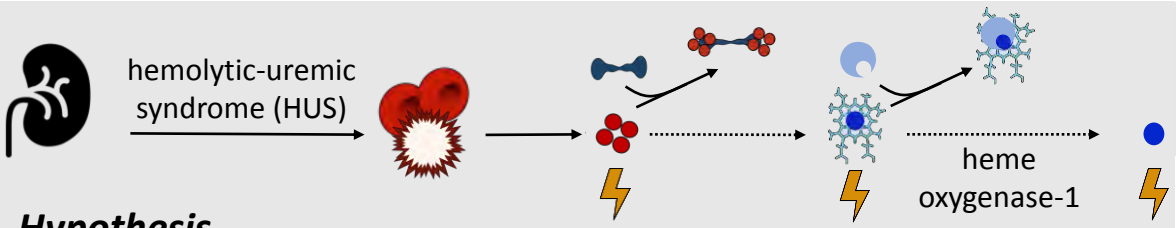

Hypothesis

The presence of Hp and Hx impacts outcome and renal pathology in HUS

Study design

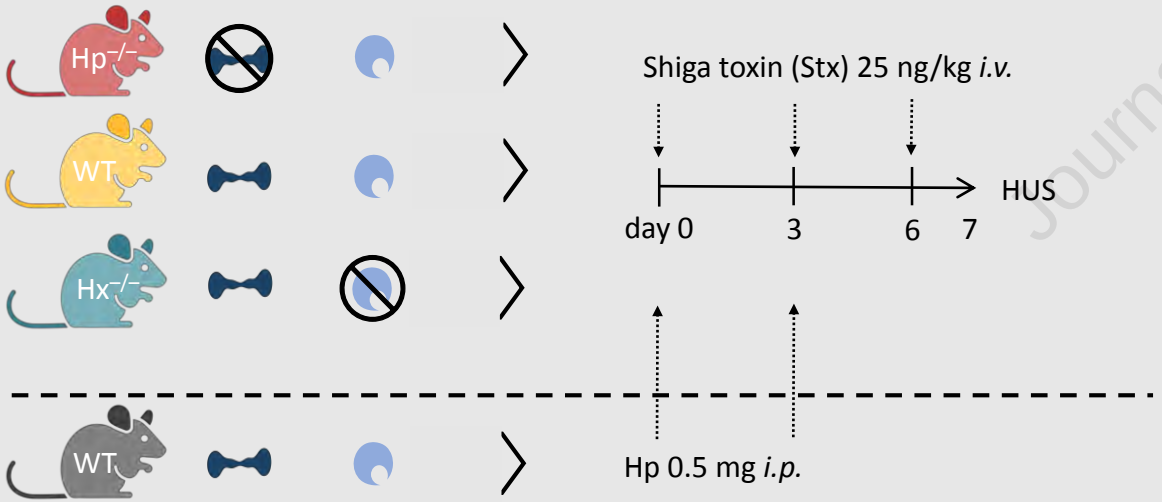

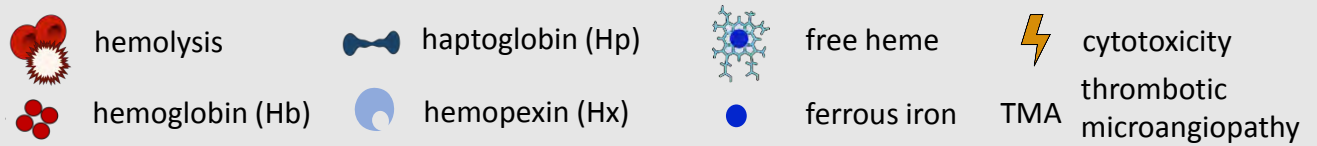

Primary outcome

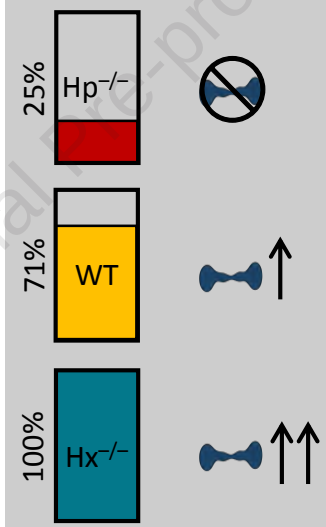

Pathological and molecular findings (day 5)

	fibrin (TMA)	platelets (TMA)	systemic hemolysis	neutrophil recruitment	tubular iron
Hp−/−	↑	↑	↑	↑	↑
WT	↔	↑	↑	↑	⊘
Hx−/−	↔	↔	↔	↔	⊘
WT + Hp	n. a.	↔	n. a.	↔	n. a.

Pirschel and Mestekemper, 2021

In mice with HUS, Hp deficiency aggravates disease progression associated with tubular iron deposition, while Hx deficiency conveys protection associated with supranormal plasma Hp, attenuated TMA and renal inflammation. Low dose Hp treatment of WT mice with HUS attenuated renal platelet deposition and neutrophil recruitment.

[QUERY TO AUTHOR: title and abstract rewritten by Editorial Office – not subject to change]

Divergent roles of haptoglobin and hemopexin deficiency for disease progression of Shiga-toxin-induced hemolytic-uremic syndrome in mice

Wiebke Pirschel, M. Sc.[1,2#], Antonio N. Mestekemper, B. A.[1,2#], Bianka Wissuwa, Ph.D.[1,2], Nadine Krieg, Ph.D.[1,2], Sarah Kröller, M. Sc.[1,2], Christoph Daniel, Prof. [3], Florian Gunzer, Prof.[4], Emanuela Tolosano, Prof. [5], Michael Bauer, Prof.[1,6], Kerstin Amann, Prof.[3], Stefan H. Heinemann, Prof.[7], and Sina M. Coldewey, Prof.[1,2,6*]

[1]Department of Anesthesiology and Intensive Care Medicine, Jena University Hospital, Jena, Germany

[2]Septomics Research Center, Jena University Hospital, Jena, Germany

[3]Department of Nephropathology, Friedrich-Alexander University (FAU) Erlangen-Nürnberg, Erlangen, Germany

[4]Department of Hospital Infection Control, University Hospital Carl Gustav Carus, TU Dresden, Dresden, Germany

[5]Department of Molecular Biotechnology and Health Sciences, Molecular Biotechnology Center, University of Torino, Torino, Italy

[6]Center for Sepsis Control and Care (CSCC), Jena University Hospital, Jena, Germany

[7]Center of Molecular Biomedicine (CMB), Department of Biophysics, Friedrich Schiller University Jena and Jena University Hospital, Jena, Germany

[#] These authors have contributed equally to this work

Running title: Haptoglobin and hemopexin in experimental HUS

abstract word count: 248/250

text word count: 4191/4000

*Correspondence:

Prof. Sina M. Coldewey, MD, PhD,

Department of Anesthesiology and Intensive Care Medicine,

Septomics Research Center,

Jena University Hospital,

Am Klinikum 1, 07747 Jena, Germany

Phone: +49 3641 9-323101

Fax: +49 3641 9-323102

sina.coldewey@med.uni-jena.de

Abstract

Thrombotic microangiopathy, hemolysis and acute kidney injury are typical clinical characteristics of hemolytic-uremic syndrome (HUS), which is predominantly caused by Shiga-toxin-producing *Escherichia coli*. Free heme aggravates organ damage in life-threatening infections, even with a low degree of systemic hemolysis. Therefore, we hypothesized that the presence of the hemoglobin- and the heme-scavenging proteins, haptoglobin and hemopexin, respectively impacts outcome and kidney pathology in HUS. Here, we investigated the effect of haptoglobin and hemopexin deficiency (haptoglobin$^{-/-}$, hemopexin$^{-/-}$) and haptoglobin treatment in a murine model of HUS-like disease. Seven-day survival was decreased in haptoglobin$^{-/-}$ (25%) compared to wild type mice (71.4%), whereas all hemopexin$^{-/-}$ mice survived. Shiga-toxin-challenged hemopexin$^{-/-}$ mice showed decreased kidney inflammation and attenuated thrombotic microangiopathy, indicated by reduced neutrophil recruitment and platelet deposition. These observations were associated with supranormal haptoglobin plasma levels in hemopexin$^{-/-}$ mice. Low dose haptoglobin administration to Shiga-toxin-challenged wild type mice attenuated kidney platelet deposition and neutrophil recruitment, suggesting that haptoglobin at least partially contributes to the beneficial effects. Surrogate parameters of hemolysis were elevated in Shiga-toxin-challenged wild type and haptoglobin$^{-/-}$ mice, while signs for hepatic hemoglobin degradation like heme oxygenase-1, ferritin and CD163 expression were only increased in Shiga-toxin-challenged wild type mice. In line with this observation, haptoglobin$^{-/-}$ mice displayed tubular iron deposition as an indicator for kidney hemoglobin degradation. Thus, haptoglobin and hemopexin deficiency play divergent roles in Shiga-toxin-mediated HUS, suggesting haptoglobin is involved, and hemopexin is redundant for the resolution of HUS pathology.

Key words

hemolytic-uremic syndrome, Shiga toxin, haptoglobin, hemopexin, iron overload, acute renal failure

Translational Statement

Hemolytic-uremic syndrome (HUS) is a life-threatening complication of infection with enterohemorrhagic *Escherichia coli* and characterized by microangiopathic hemolytic anemia and renal impairment. Evidence suggests that free heme contributes to disease progression in systemic inflammation. We show that the hemoglobin and heme scavenger proteins haptoglobin and hemopexin play divergent roles in HUS pathogenesis: Our data indicate that hemopexin is redundant for the resolution of HUS pathology, while haptoglobin deficiency aggravates disease progression in mice with HUS and higher endogenous haptoglobin levels as well as haptoglobin administration are associated with an attenuation of surrogate parameters of thrombotic microangiopathy and inflammation. (98/100)

Introduction

The hemolytic-uremic syndrome (HUS) is a rare but severe systemic complication upon infection with Shiga-toxin (Stx)-producing enterohemorrhagic *Escherichia coli* (STEC). STEC-HUS, a thrombotic microangiopathy (TMA) primarily affecting the kidneys, is clinically characterized by hemolytic anemia, thrombocytopenia and end-organ damage caused by thrombosis in small blood vessels.[1] It is the most frequent reason for acute kidney injury (AKI) in childhood,[2] but severe HUS courses have also been described in adults.[3, 4] Although the pathogenesis is still under investigation,[5] it is evident that Stx, comprising Stx1 and Stx2, is the major virulence factor of STEC.[6] By binding to globotriaosylceramide (Gb3) receptor with high affinity and interfering with protein synthesis, Stx leads to epithelial and endothelial cell damage thereby initiating the occurrence of renal TMA.[6] Clot deposition in the microvasculature leads to subsequent tissue ischemia, organ injury, and hemolysis.[1, 6] Therapeutic options are currently supportive and dialysis is often required. Since there is no specific therapy, further studies are needed to evaluate potential targets for therapeutic approaches. Free heme is a known relevant factor in the maintenance of pathological processes in life-threatening infections by leading to inflammation,[7, 8] complement activation[9, 10] and reactive oxygen species (ROS).[11] Recently, elevated free heme could be detected in plasma of STEC-HUS patients.[12] However, the impact of heme and heme degradation products on disease progression has not yet been investigated. In mammalians, clearance of cell-free hemoglobin (Hb) and heme-bound iron is mainly regulated by the scavenging systems haptoglobin (Hp) and hemopexin (Hx). Hp is the plasma protein with the highest binding affinity to Hb. As an acute-phase protein it is upregulated under inflammatory conditions and predominantly produced in hepatocytes.[13] Key functions of Hp are preventing glomerular filtration of Hb and enabling Hb degradation by the reticuloendothelial system, especially in spleen and liver,[14, 15] thereby protecting the kidney from Hb-mediated cytotoxicity.[16] CD163, a membrane receptor on macrophages, binds to the Hp-Hb complex with high affinity and leads to its endocytosis.[15] In the absence of Hp, glomerular filtered Hb binds to the multiligand receptors megalin and cubilin mediating its tubular uptake.[17] When Hb becomes oxidized to methemoglobin, its heme groups dissociate and potentially exert cytotoxicity via the centrally bound iron.[18] Various plasma proteins, such as albumin, α1-microglobulin (α1M) and Hx prevent iron-mediated damage by binding free heme.[18] Hx is the scavenging protein with the highest affinity to heme and a murine but not human acute-phase protein mainly produced in the liver.[19, 20] The Hx-heme complex is removed from plasma by low-density lipoprotein(LDL)-receptor related protein

1-mediated endocytosis.[21] After its uptake, the intracellular degradation of heme into equimolar amounts of ferrous iron (Fe^{2+}), carbon monoxide (CO), and biliverdin is mediated via the two heme oxygenase isoforms (HO-1, HO-2).[22] HO-1 is ubiquitously expressed, inducible, and gains cytoprotective properties by modulating the tissue response in the presence of various stress factors.[22] First evidence from cell-culture experiments suggest that Stx augments hemin-mediated toxicity in renal epithelial cells which can be attenuated by HO-1 induction.[23] Heme degradation by HO-1 increases the availability of free iron.[24] While biliverdin is converted to bilirubin by biliverdin reductase,[25] labile iron is rapidly bound by the intracellular iron-storage protein ferritin to prevent ROS formation.[26] Ferritin consists of a heavy (Fth1) and a light (Ftl1) chain, the former has ferroxidase activity being crucial for iron storage.[27] The transmembrane protein ferroportin (SCL40A1) mediates iron transport into the circulation where it is bound by transferrin.[28] Ferroportin expression is locally regulated by iron-regulatory proteins and systemically by the acute-phase protein hepcidin.[28]

Hitherto, the role of the Hb- and heme-scavenging proteins Hp and Hx in HUS pathology has not been addressed. We hypothesized, that Hp and Hx impact disease progression of STEC-HUS by ameliorating Hb- and heme-mediated cytotoxicity and kidney injury. Thus, we analyzed the effect of Hp and Hx deficiency as well as Hp treatment in a murine model of HUS-like disease. Elucidating the role of these proteins in STEC-HUS provides a deeper understanding of the pathogenesis and offers the potential to develop novel therapeutic strategies.

Methods

Information on commercially available kits, buffers, antibodies employed in the study and other methodical details including methods relevant to supplementary results are provided in the supplement.

Animal experiments

Generation of the $Hp^{-/-}$ and $Hx^{-/-}$ mice was described in [29] and [16], respectively. HUS was induced in 10-15 weeks old male C57BL/6J wild-type (WT), $Hp^{-/-}$ and $Hx^{-/-}$ mice.[30] Mice were subjected to 25 ng/kg bodyweight (BW) Stx2 (WT Stx, $Hp^{-/-}$ Stx, $Hx^{-/-}$ Stx) or 0.9% NaCl (WT sham, $Hp^{-/-}$ sham, $Hx^{-/-}$ sham) intravenously (*i.v.)* on days 0, 3 and 6 accompanied by volume resuscitation with 800 µl Ringer´s lactate subcutaneously (*s.c.)* three times daily. BW and HUS score (supplementary Table S1) were determined as described previously.[30] Survival was assessed up to day 7 or mice were sacrificed when an HUS score of 4 (high-grade disease state) was reached to comply with ethical regulations. All further analyses were performed in samples obtained at day 5 after HUS induction. For Hp treatment WT mice received

0.5 mg Hp (ABIN491578, antibodies-online GmbH) in 200 µl PBS intraperitoneally (*i.p.*) on day 0 and 3. All procedures were approved by the regional animal welfare committee (Thuringian State Office for Consumer Protection, Bad Langensalza, Germany; registration number 02-040/16) and performed in accordance with the German legislation.

Plasma analysis

Blood withdrawal, plasma preparation and analysis of hemolysis were performed as described previously.[30] Plasma α1M, albumin, Hp, Hx, urea, neutrophil gelatinase-associated lipocalin (NGAL), bilirubin and hepcidin were analyzed with commercial kits according to manufactures instructions (supplementary Table S2).

Histological and immunohistochemical analysis

Kidneys were histopathologically and immunohistochemically evaluated using periodic acid Schiff (PAS), kidney injury molecule-1 (KIM-1), CD31, F4-80, complement component 3 (C3c), cleaved caspase-3 (CC-3) staining as described previously,[30] as well as ferroportin, lymphocyte antigen 6 complex, locus G (Ly6G), glycoprotein 1b (GP1b) and iron staining (antibodies in supplementary Table S3, 4).

Gene expression analysis

Isolation of RNA, performance of real-time PCR (supplementary Table S5) and data analysis were described previously.[31, 32]

Protein expression analysis

Immunoblot analysis was performed as described previously.[31] For blotting of renal HO-1 100 µg and for Fth1, hepatic HO-1 and CD163 25 µg of total protein were used (antibodies in supplementary Table S6). Proteins of interest were normalized to total protein load using the stain-free technology (Bio-Rad Laboratories, Inc.). Bands with normalization factors less than 0.7 and more than 1.3 were excluded from analysis.[33] Samples from 6 animals per group were pooled to equal protein amounts for the representative blots of renal HO-1 and Fth1. Individual blots (1 animal/group) are shown in supplementary Figure S1. Data are presented relative to the mean of sham animals.

Statistics

Data were analyzed with GraphPad Prism 7.03 and are depicted as median ± interquartile range (IQR) for n observations. Survival was analyzed generating Kaplan-Meier curves and evaluated by Mantel-Cox test. Mann-Whitney *U*-test was used to compare the Stx groups of each strain with the corresponding

sham group, each knockout sham group to the WT sham group and each knockout Stx group to the WT Stx group. A *P*-value < 0.05 was considered significant.

Data sharing statement

For original data, please contact sina.coldewey@med.uni-jena.de

Results

SEVEN-DAY SURVIVAL IS WORSE IN HP$^{-/-}$ AND IMPROVED IN HX$^{-/-}$ MICE

Survival rate of Stx-challenged WT mice (71.4%) was decreased but not significantly altered compared to WT sham mice (100%) (Figure 1a). Seven-day survival of Stx-challenged Hp$^{-/-}$ mice (25%) was lower compared to Hp$^{-/-}$ sham mice (100%). Most notably, all Stx-challenged Hx$^{-/-}$ mice survived (100%). Both, Stx-challenged WT and Hx$^{-/-}$ mice, showed significantly higher survival rates compared to Stx-challenged Hp$^{-/-}$ mice.

THE COURSE OF DISEASE IS MORE SEVERE IN HP$^{-/-}$ AND WT MICE THAN IN HX$^{-/-}$ MICE

Disease progression, indicated by increased HUS scores, was apparent in all Stx-challenged mice (Figure 1b). However, while HUS scores of Stx-challenged Hp$^{-/-}$ and WT mice were comparable on day 5, Stx-challenged Hx$^{-/-}$ mice showed less disease progression (Figure 1c). All Stx-challenged mice lost weight during the course of disease (Figure 1d). Five days after HUS induction, weight loss of Hp$^{-/-}$ mice was higher compared to WT mice, while weight loss of Hx$^{-/-}$ mice was comparable to WT mice (Figure 1e).

EXPRESSION OF THE HB AND HEME SCAVENGER PROTEINS HX, α1M, ALBUMIN AND HP IN WT, HP$^{-/-}$ AND HX$^{-/-}$ MICE

A compensatory upregulation of α1M in Hx$^{-/-}$ mice with sickle cell disease[34] as well as Hp in Hx$^{-/-}$ mice and Hx in Hp$^{-/-}$ mice with artificial hemolysis has been described.[35] Thus, we investigated plasma levels of Hb- and heme-binding proteins.

Hepatic *Hx* gene expression was increased in Stx-challenged WT and Hp$^{-/-}$ mice compared to their corresponding sham group (Figure 2a). A similar pattern was found for Hx plasma levels, they were higher in Hp$^{-/-}$ sham mice compared to WT sham mice (Figure 2b).

Plasma α1M was decreased in Stx-challenged WT but unchanged in Hp$^{-/-}$ and Hx$^{-/-}$ mice compared to their corresponding sham group (Figure 2c).

Heme-binding properties have been described for albumin.[36] However, plasma albumin was unchanged in Stx-challenged WT and knockout mice compared to their corresponding sham group (Figure 2d). Hepatic *Hp* gene expression was increased in Stx-challenged WT and $Hx^{-/-}$ mice compared to their corresponding sham group (Figure 2e). A similar pattern was found for plasma Hp (Figure 2f). Notably, plasma Hp was higher in $Hx^{-/-}$ compared to WT mice irrespective of Stx challenge.

RENAL IMPAIRMENT IN WT, $HP^{-/-}$ AND $HX^{-/-}$ MICE

Liver, lung, colon and kidneys of WT, $Hp^{-/-}$, and $Hx^{-/-}$ mice were assessed for morphological alterations. While no relevant morphological changes appeared in lung and colon, diffuse granulomatous changes were detected in liver sections of Stx-challenged mice and knockout sham animals (supplementary Figure S2, 3), accompanied by unchanged liver enzymes (supplementary Figure S4).

All Stx-challenged genotypes showed severe renal injury, indicated by increased plasma urea (Figure 3a) and NGAL (Figure 3b), altered morphology in PAS-stained sections (Figure 3c, supplementary Figure S5A) and elevated KIM-1 expression (Figure 3d), suggesting that the kidney is the primarily affected organ in this murine model. Plasma creatinine was elevated in all Stx-challenged genotypes compared to their corresponding sham group, and slightly increased in Stx-challenged $Hp^{-/-}$ compared to WT mice (supplementary Figure S6A). Potassium plasma levels were elevated in Stx-challenged WT and $Hp^{-/-}$ but not in $Hx^{-/-}$ mice compared to their corresponding sham group (supplementary Figure S6B). Furthermore, enhanced potassium levels were observed in Stx-challenged $Hp^{-/-}$ compared to WT mice.

In human STEC-HUS, glomerular damage is predominant, but tubular damage also contributes to the pathology.[37] Ultrastructural analysis revealed severe tubular injury in all Stx-challenged mice but no alterations of podocytes (supplementary Figure S7). Murine Stx models do not completely reconstruct human HUS. Several models have been developed to highlight certain aspects of HUS, comprising genetic modifications to study the lectin pathway[38] or enhance thrombotic processes[39] and co-injection of LPS to provoke broader HUS symptoms like glomerular changes and thrombocytopenia.[40] This study focuses on Stx-mediated pathomechanisms.

Renal endothelial cells are the main target of Stx by binding Gb3-receptors[6] and apoptotic cells are increased in kidneys of STEC-HUS patients.[37] A comparable loss of endothelial cells in all Stx-challenged genotypes indicated by CD31 expression (Figure 3e, supplementary Figure S5B), and raised apoptosis indicated by CC-3 expression (Figure 3f, supplementary Figure S5C) compared to their

corresponding sham group was observed. Compared to Stx-challenged WT mice, $Hx^{-/-}$ mice expressed less CC-3.

Renal HO-1 expression was increased in Stx-challenged strains compared to their corresponding sham group (Figure 3g, supplementary Figure S1A). Interestingly, HO-1 levels were the highest in Stx-challenged $Hp^{-/-}$ (15-fold), followed by WT mice (10-fold) whereas $Hx^{-/-}$ mice (6-fold) had the lowest levels.

Renal microthrombi formation is a hallmark of HUS pathology. Fibrin deposition was detected by SFOG staining in all Stx-challenged $Hp^{-/-}$ mice but only in some Stx-challenged WT and $Hx^{-/-}$ mice (supplementary Figure S8).

Increased numbers of renal GP1b-positive thrombocytes were observed in Stx-challenged WT and $Hp^{-/-}$ but not in $Hx^{-/-}$ mice compared to their corresponding sham group (Figure 3h).

ELEVATED HEMOLYSIS IN WT AND $HP^{-/-}$ MICE

Increased hemolysis and plasma bilirubin were detected in Stx-challenged WT and $Hp^{-/-}$ but not in $Hx^{-/-}$ mice compared to their corresponding sham group (Figure 4a-b). Hepatic and renal gene expression of proteins taking part in heme and iron homeostasis displayed varying regulations (supplementary Figure S9, 10). Hepatic *Hmox1* expression (Figure 4c) as well as levels of hepatic HO-1, Fth1, and CD163 were elevated in Stx-challenged WT but not in $Hp^{-/-}$ and $Hx^{-/-}$ mice compared to their corresponding sham group (Figure 4d-l).

RENAL INFLAMMATION IS ATTENUATED IN $HX^{-/-}$ MICE

Macrophage[37] and neutrophil[41] recruitment to kidneys of STEC-HUS patients has been described and neutrophilia was shown to be associated with poor prognosis.[42, 43] F4-80-positive macrophages were increased in kidneys of Stx-challenged WT and $Hp^{-/-}$ but not in $Hx^{-/-}$ mice compared to their corresponding sham group (Figure 5a). F4-80 expression was elevated in $Hp^{-/-}$ sham compared to WT sham mice. Macrophages were decreased in Stx-challenged $Hp^{-/-}$ and $Hx^{-/-}$ compared to WT mice.

Ly6G expression, indicating neutrophil granulocyte recruitment, was elevated in kidneys of Stx-challenged WT and $Hp^{-/-}$ but not in $Hx^{-/-}$ mice compared to their corresponding sham group (Figure 5b).

C3c deposition, indicating complement activation, was increased in all Stx-challenged mice compared to their corresponding sham group. C3c expression was elevated in Stx-challenged $Hp^{-/-}$ compared to WT mice (Figure 5c).

HP INTERVENTION IN WT MICE

Stx-challenged WT mice received a low dose Hp, which has been reported to be beneficial in septic mice,[44] to evaluate its protective function in HUS-like disease (Figure 6a). Stx groups showed enhanced plasma NGAL, altered renal morphology, increased expression of KIM-1, CC-3 and F4-80-positive macrophages, C3c in the kidneys compared to their corresponding sham groups (Figure 6b-g). Renal GP1b and Ly6g expression was elevated in the Stx-challenged vehicle group but not in Hp-treated mice with HUS compared to the corresponding control group (Figure 6h-i). Hp-treated mice with HUS showed decreased Ly6g expression compared to the corresponding vehicle group (Figure 6i).

TUBULAR IRON DEPOSITION IS INCREASED IN $Hp^{-/-}$ MICE BUT NOT IN WT AND $Hx^{-/-}$ MICE

Hp and Hx take part in iron homeostasis by their scavenging function regarding Hb and heme-bound iron. Pronounced iron deposition was detected in tubules of the $Hp^{-/-}$ but not in the WT and $Hx^{-/-}$ strain, irrespective of treatment (Figure 7a). Iron-positive tubules were increased in Stx-challenged $Hp^{-/-}$ mice compared to their corresponding sham group. In accordance, highest renal Fth1 expression was found in $Hp^{-/-}$, followed by $Hx^{-/-}$ mice, whereas WT mice had the lowest levels (Figure 7b). Fth1 expression was slightly elevated in all Stx-challenged mice compared to their corresponding sham group.

We analyzed DMT1, megalin and cubilin which are responsible for cellular uptake of iron[45] and Hb respectively.[46] DMT1 expression was reduced in Stx-challenged $Hx^{-/-}$ but not in WT and $Hp^{-/-}$ mice compared to their corresponding sham group (supplementary Figure S11A). Megalin and cubilin expression was high in all genotypes independent of Stx challenge (supplementary Figure S11B-C).

Plasma Hepcidin was increased in all Stx-challenged mice compared to their corresponding sham group (Figure 7c). In Stx-challenged $Hp^{-/-}$ mice, hepcidin levels were elevated compared to WT Stx mice. Ferroportin-positive tubules were decreased in all Stx-challenged genotypes compared to their corresponding sham group (Figure 7d), in Stx-challenged $Hp^{-/-}$ compared to WT mice and in $Hp^{-/-}$ sham compared to WT sham mice.

Renal MDA, nitrotyrosine and NOX-1 were investigated as markers for oxidative stress. MDA was enhanced in $Hp^{-/-}$ compared to WT mice, independent of Stx challenge. Nitrotyrosine and NOX-1 expression were increased in Stx-challenged $Hp^{-/-}$ compared to WT mice (supplementary Figure S12).

Discussion

We showed that Hp and Hx play divergent roles for disease progression in HUS, indicated by a survival advantage of $Hx^{-/-}$ mice and a higher mortality rate in $Hp^{-/-}$ mice compared to WT mice. Albeit the role of Hx in infectious diseases is discussed controversially, we hypothesized that both scavenger proteins

287 are required for the resolution of HUS pathology, accompanied by hemolysis. Thus, the survival benefit
288 of $Hx^{-/-}$ mice appeared unexpected to us, in particular, as Hx administration has been described to be
289 protective in a murine model of sepsis, with a moderate degree of hemolysis[8] as well as during severe
290 hemolysis.[7] However, in line with our results, Spiller *et al.* showed that Hx deficiency was protective in
291 septic mice.[47] The high mortality rate of $Hp^{-/-}$ mice with HUS was consistent with previously reported
292 aggravated vulnerability under hemolytic[29], inflammatory[48], and septic[44] conditions and emphasizes the
293 physiological relevance of Hp in diseases accompanied by hemolysis.
294 To evaluate possible mechanisms underlying the observed outcome of mice with HUS, we assessed
295 various organ systems, such as kidneys, liver, lung and colon for pathological changes. We only found
296 obvious morphological alterations in kidneys of Stx-challenged mice.
297 Acute TMA-derived hemolysis is a disease-defining feature in patients with STEC-HUS.[49] Renal fibrin
298 deposition was present in some $Hx^{-/-}$ and WT mice with HUS. However, unlike in Stx-challenged WT
299 mice, renal platelet deposition as surrogate parameter of TMA was not significantly increased in Stx-
300 challenged $Hx^{-/-}$ mice compared to the corresponding sham group. These findings indicate attenuated
301 TMA in Stx-challenged $Hx^{-/-}$ mice. Furthermore, renal apoptosis as well as HO-1 expression, as
302 surrogate parameter for inflammation,[50] hypoxia,[51] and accumulation of heme[52], were less pronounced
303 in $Hx^{-/-}$ compared to WT mice with HUS. In line with this, we found a moderate hemolysis, increased
304 bilirubin levels in WT but not in $Hx^{-/-}$ mice with HUS. Consequently, we observed an induction of hepatic
305 HO-1, Fth1, and CD163 in Stx-challenged WT but not in $Hx^{-/-}$ mice, most likely indicating the clearance
306 of Hp-Hb complexes by liver macrophages via CD163.[15, 53] Of note, in patients with HUS, high plasma
307 heme has been reported to be associated with high plasma HO-1 levels.[12]
308 It has been reported that Stx- and heme-mediated cytotoxicity is sensitized by inflammation.[54, 55]
309 Furthermore, renal macrophage[37] and neutrophil recruitment[41] are observed in renal biopsies of STEC-
310 HUS patients. In Stx-challenged $Hx^{-/-}$ mice, renal inflammation was less pronounced. This was indicated
311 by a reduced macrophage expression compared to Stx-challenged WT mice and by an attenuated
312 neutrophil expression. Considering our results, we conclude that Hx deficiency improves the survival of
313 mice with HUS by ameliorating renal pathology and consequently reducing fatal events resulting from
314 end stage kidney disease.
315 $Hx^{-/-}$ mice with or without artificial hemolysis have been described to display higher endogenous Hp
316 levels.[35] We could reproduce this finding in $Hx^{-/-}$ mice with or without HUS. Unlike STEC-HUS patients,
317 who often display depleted Hp levels[12] most likely as a sign of plasma Hp consumption, the acute-phase

reaction with high Hp expression seems to predominate in mice with HUS. A variety of anti-inflammatory and immunomodulatory functions of Hp have been reported, such as inhibiting calcium influx and subsequent oxidative burst by binding to activated neutrophils[56] and suppressing LPS-induced TNF-α production of macrophages.[48] Therefore, we hypothesized that increased Hp plasma levels in $Hx^{-/-}$ compared to WT mice might contribute to the protective effects of the constitutional Hx knockout. Treatment of Stx-challenged WT mice with low dose Hp attenuated renal platelet deposition and neutrophil recruitment. Interestingly, it has been shown recently that reduction of neutrophil recruitment to kidneys of WT mice by inhibition of CXC chemokine receptor 2 conveys renal protection.[57] However, as low dose Hp administration did not attenuate renal injury and CC-3 expression, our results indicate that the elevated endogenous Hp expression in $Hx^{-/-}$ mice alone does not explain all beneficial effects observed in these mice.

We further investigated the impact of Hp deficiency on renal pathology. We identified similar patterns of tubular damage and renal thrombocyte depositions in $Hp^{-/-}$ and WT mice with HUS. This is consistent with findings of Fagoonee *et al.* showing no differences in renal injury between $Hp^{-/-}$ and WT mice subjected to ischemia reperfusion injury (IRI).[46] But renal fibrin deposition indicating microthrombi formation, a surrogate parameter for TMA, was increased in Stx-challenged $Hp^{-/-}$ compared to WT mice. Interestingly, Hx plasma levels were higher in $Hp^{-/-}$ sham compared to WT sham mice, suggesting a compensatory adaptation of the Hp deficient genotype. After Stx challenge, plasma Hx increased in WT and even further in $Hp^{-/-}$ mice, suggesting that, similar to Hp, rather the acute-phase reaction then the Hx consumption prevails in mice with HUS. However, in STEC-HUS patient with hemolysis Hx depletion has been reported.[12] There is first evidence that Hx can cause a nephrin-dependent remodeling of the actin cytoskeleton in podocytes[58], which is supported by the observation that unilateral renal infusion of rats with Hx leads to glomerular alterations with concomitant proteinuria.[59, 60] In our studies, we detected no ultrastructural changes of podocytes independent of genotype or intervention. Assumably, the increase of Hx reflects a compensatory mechanism to detoxify heme in the absence of Hp and/or in Stx-induced HUS-like disease with a moderate degree of hemolysis.

We observed a disturbed iron homeostasis, elevated markers of oxidative stress and increased renal complement activation in kidneys of Stx-challenged $Hp^{-/-}$ compared to WT mice, which might explain the detrimental survival of $Hp^{-/-}$ mice with HUS.

Specifically, we found not only elevated plasma hepcidin and decreased renal ferroportin levels in Stx-challenged $Hp^{-/-}$ compared to WT mice, but also tubular iron deposition in $Hp^{-/-}$ sham mice, that further

increased following Stx challenge. In line with this observation, a strong enhancement of Hb-derived iron in tubules of adult $Hp^{-/-}$ sham mice has been described to accumulate with age and after IRI.[46] Other studies showed nephrotoxic effects in experimental hemochromatosis[61] or chronic hemosiderosis in rats.[62] Thus, the observed iron deposition is likely to contribute to the detrimental outcome of Stx-challenged $Hp^{-/-}$ mice. To date, there are no studies examining iron homeostasis in STEC-HUS patients. However, a study analyzing genetic polymorphisms in STEC-HUS patients suggests that genes encoding for proteins involved in iron transport might influence the host susceptibility to develop HUS.[63] There is increasing evidence that in the absence of Hp, Hb is glomerular filtrated and that the tubular uptake through megalin and cubilin prevents urinary iron loss.[17, 64] We observed elevated renal HO-1 expression and acute tubular iron deposition in Stx-challenged $Hp^{-/-}$ mice, indicating alterations in renal heme and iron homeostasis. Unlike in WT mice, we found no induction of hepatic HO-1, Fth1, and CD163 in Stx-challenged $Hp^{-/-}$ mice, suggesting that Hb cannot be cleared by liver macrophages via CD163 due to the Hp deficiency. In hemolytic disease, it has been shown that liver macrophages can switch to a proinflammatory phenotype in the presence of heme and iron.[7] In this study, we did not characterize the macrophage phenotype. However, quantitatively, renal macrophage recruitment was surprisingly attenuated in Stx-challenged $Hp^{-/-}$ compared to WT mice.

Furthermore, markers of oxidative stress were elevated in Stx-challenged $Hp^{-/-}$ compared to WT mice. This finding might result from the observed tubular iron increase, as it has been described that heme-bound iron is a potent mediator for ROS generation which can lead to ferroptosis[65] and has been associated to thrombocyte activation *in vitro*.[66] In patients with HUS, enhanced lipid oxidation as marker for oxidative stress has been shown to be increased and linked to hemolysis.[67]

There is evidence, that complement activation occurs in the presence of heme in models of artificial hemolysis[10] and sickle cell disease.[9] Increased complement activation in the plasma of STEC-HUS patients has been described,[68] and preclinical studies suggest that this activation might lead to an aggravation of HUS pathology.[69-71] In accordance, we found elevated renal C3c deposition in $Hp^{-/-}$ compared to WT mice with HUS.

We conclude, that Hp and Hx deficiency play divergent roles for HUS disease progression in mice. While Stx-challenged $Hx^{-/-}$ mice were characterized by less disease severity and an attenuated renal pathology, $Hp^{-/-}$ mice displayed a higher mortality rate, accompanied by renal iron and complement deposition. Low dose Hp treatment of Stx-challenged WT mice attenuated surrogate parameters of renal

TMA and inflammation, but not kidney injury. Thus, we suggest, that Hp-dependent mechanisms convey – at least in part – protection and that Hp is important for the resolution of STEC-HUS pathology.

Disclosures

The authors have no conflict of interest to declare.

Authorship Contribution

SMC designed, planned and supervised the study. SMC, WP, ANM wrote the manuscript and the revisions. WP, BW performed animal experiments with WT, $Hp^{-/-}$, $Hx^{-/-}$ mice, including data analysis. SK, BW, NK performed animal experiments with Hp administration including data analysis. WP, ANM analyzed ELISA data. WP, SK, ANM performed histology and immunohistochemistry including data analysis. ANM performed gene expression, western blot analyses and hemolysis assay including data analysis. FG provided Shiga toxin. CD, KA planned and supervised histology for liver, lung and colon, immunohistochemistry for GP1b, electron microscopy and analyzed corresponding data. SMC, WP, ANM, BW, NK, SK, CD, FG, ET, MB, KA and SHH provided important intellectual content and revised the manuscript. All authors carefully reviewed and approved the manuscript.

Supplementary Material

Supplementary File (PDF)

Supplementary Methods.

Table S1. HUS score

Table S2. Commercial Kits

Table S3. Primary antibodies used for immunohistochemistry

Table S4. Secondary antibodies used for immunohistochemistry

Table S5. Primer used for quantitative real-time PCR

Table S6. Primary and secondary antibodies used for western blot analyses

Supplementary Results.

Supplementary Figures.

Figure S1.

Supplementary Figure S1. Renal protein expression of HO-1 and Fth1 in WT, $Hp^{-/-}$ and $Hx^{-/-}$ mice with experimental HUS. Protein expression on day 5 of (A) HO-1 (28 kDa) and (B) Fth1 (21 kDa) in

kidneys of sham mice and mice subjected to Stx. Each line represents a single blot of indicated strains and groups. Fth1, ferritin heavy chain; Hp, haptoglobin; HO-1, heme oxygenase-1; Hx, hemopexin; Stx, Shiga toxin; WT, wild type. Representative blots of pooled samples are shown in Figure 3g (HO-1) and Figure 7b (Fth1).

Figure S2.

Supplemental Figure S2. Granulomatous alterations in the liver of WT, Hp$^{-/-}$ and Hx$^{-/-}$ mice with experimental HUS. Quantification and representative pictures of H&E staining in liver sections on day 5 of sham mice and mice subjected to Stx (n = 6 per group). Bars = 500 µm. Data are expressed as scatter dot plot with median ± IQR for n observations. *P < 0.05 vs. corresponding sham group, $^{\#}P$ < 0.05 vs. WT sham group (Mann-Whitney *U*-test). Hp, haptoglobin; H&E, hematoxylin and eosin; Hx, hemopexin; IQR, interquartile range; Stx, Shiga toxin, WT, wild type.

Figure S3.

Supplemental Figure S3. Inflammatory alterations in lung and colon of WT, Hp$^{-/-}$ and Hx$^{-/-}$ mice with experimental HUS. Representative pictures of (A) PAS reaction in lungs and (B) H&E staining in colon sections on day 5 of sham mice and mice subjected to Stx (n = 6 per group). (A) Bars = 200 µm (B) Bars = 500 µm. Since no morphological changes were observed in the intestine and lung, only the presence of inflammatory cell aggregates was determined for these two organs (0 = absent; 1 = present). Few inflammatory cell aggregates were observed in the lung of WT sham (1/6), WT Stx (3/6), Hp$^{-/-}$ sham (2/6), Hp$^{-/-}$ Stx (2/6), Hx$^{-/-}$ sham (3/6), and Hx$^{-/-}$ Stx (3/6) mice. Few inflammatory cell aggregates were observed in the colon of WT sham (2/6), WT Stx (1/6), Hp$^{-/-}$ sham (4/6), Hp$^{-/-}$ Stx (3/6), Hx$^{-/-}$ sham (0/6), and Hx$^{-/-}$ Stx (2/6) mice. Hp, haptoglobin; H&E, hematoxylin and eosin; Hx, hemopexin; IQR, interquartile range; PAS, periodic acid Schiff; Stx, Shiga toxin, WT, wild type.

Figure S4.

Supplementary Figure S4. Plasma values of ALAT and ASAT in WT, Hp$^{-/-}$ and Hx$^{-/-}$ mice with experimental HUS. Determination of plasma (A) ALAT (WT sham: n = 12; WT Stx, Hp$^{-/-}$ sham and Stx, Hx$^{-/-}$ Stx: n = 6, sham; Hx$^{-/-}$: n = 5) and (B) ASAT (n = 12 per group) in sham mice and mice subjected to Stx on day 5. (A-B) Data are expressed as scatter dot plot with median ± IQR for n observations.

*P < 0.05, vs. corresponding sham group, $^{\#}P$ < 0.05 vs. WT sham group (Mann-Whitney *U*-test). ALAT, alanine aminotransferase; ASAT, aspartate aminotransferase; Hp, haptoglobin; Hx, hemopexin; IQR, interquartile range; Stx, Shiga toxin; WT, wild type.

Figure S5.

Supplementary Figure S5. Renal PAS reaction, CD31 and CC-3 staining in WT, Hp$^{-/-}$ and Hx$^{-/-}$ mice with experimental HUS. Representative pictures on day 5 of (A) PAS reaction, immunohistochemical (B) CD31 and (C) CC-3 staining in renal sections of sham mice and mice subjected to Stx (n = 8 per group). Bars = 100 µm. (A-C) Quantifications are shown in Figures 3c (PAS), 3e (CD31) and 3f (CC-3). CC-3, cleaved caspase-3; Hp, haptoglobin; Hx, hemopexin; PAS, periodic acid Schiff; Stx, Shiga toxin, WT, wild type.

Figure S6.

Supplementary Figure S6. Kidney dysfunction in WT, Hp$^{-/-}$ and Hx$^{-/-}$ mice with experimental HUS. Determination of (A) creatinine and (B) potassium in plasma of sham mice and mice subjected to Stx (n = 8 per group). (A-B) Data are expressed as scatter dot plot with median ± IQR for n observations. *P < 0.05, vs. corresponding sham group, $^{\S}P$ < 0.05 vs. WT Stx group (Mann-Whitney *U*-test). Hp, haptoglobin; Hx, hemopexin; Stx, Shiga toxin, WT, wild type.

Figure S7.

Supplementary Figure S7. Electron microscopic analysis of kidney tissue from WT, Hp$^{-/-}$ and Hx$^{-/-}$ mice with experimental HUS. Representative ultrastructural images on day 5 of sham mice and mice subjected to Stx. After HUS induction, only occasional widening of the podocyte foot processes (FP) and slightly swollen endothelium were observed in all genotypes. The fenestration of the endothelium (EC) was not noticeably altered due to Stx challenge. The glomerular basement membranes were neither widened nor injured and mesangial cells appeared normal (N = nucleus; P = podocyte; RBC = red blood cell). Scale bar = 1 µm. Hp, haptoglobin; Hx, hemopexin; Stx, Shiga toxin; WT, wild type.

Figure S8.

Supplementary Figure S8. Renal fibrin depositions in WT, Hp$^{-/-}$ and Hx$^{-/-}$ mice with experimental HUS. Quantifications and representative pictures of SGOF staining on day 5 in renal sections of sham mice and mice subjected to Stx (n = 8 per group). Data are expressed as scatter dot plot with median ± IQR for n observations. *P < 0.05, vs. corresponding sham group, $^{§}P$ < 0.05 vs. WT Stx group (Mann-Whitney *U*-test). Hp, haptoglobin; Hx, hemopexin; IQR, interquartile range; SFOG; acid fuchsin orange G; Stx, Shiga toxin, WT, wild type.

Figure S9.

Supplementary Figure S9. Hepatic heme and iron metabolism in WT, Hp$^{-/-}$ and Hx$^{-/-}$ mice with experimental HUS. mRNA expression of (A) *CD163,* (B) *Trf*, (C) *Lrp1*, (D) *Fth1*, (E) *Ftl1,* (F) *Alb* and (G) *SCL40A1* in livers of sham mice and mice subjected to Stx (n = 6 per group). (A-H) Data are expressed as scatter dot plot with median ± IQR for n observations. *P < 0.05 vs. corresponding sham group, $^{#}P$ < 0.05 vs. WT sham group, $^{§}P$ < 0.05 vs. WT Stx group (Mann-Whitney *U*-test). *Alb*, albumin; *Fth1*, ferritin heavy chain; *Ftl1*, ferritin light chain; Hp, haptoglobin; *Hmox1*, heme oxygenase-1; Hx, hemopexin*;* IQR, interquartile range; *Lrp1*, LDL-receptor related protein 1; *Trf*, transferrin; *SCL40A1*, ferroportin; Stx, Shiga toxin; WT, wild type.

Figure S10.

Supplementary Figure S10. Renal heme and iron metabolism in WT, Hp$^{-/-}$ and Hx$^{-/-}$ mice with experimental HUS. mRNA expression of (A) *Alb*, (B) *Trf*, (C) *SCL40A1* (D) *Lrp1*, (E) *Ftl1,* (F) *Fth1,* (G) *Lrp,* (H) *Cubn* and (I) *Hmox1* on day 5 in kidneys of sham mice and mice subjected to Stx (n = 6 per group). (A-I) Data are expressed as scatter dot plot with median ± IQR for n observations. *P < 0.05 vs. corresponding sham group, $^{#}P$ < 0.05 vs. WT sham group, $^{§}P$ < 0.05 vs. WT Stx group (Mann-Whitney *U*-test). *Alb*, albumin; *Cubn,* cubilin*; Fth1,* ferritin heavy chain; *Ftl1*, ferritin light chain; Hp, haptoglobin; *Hmox1*, heme oxygenase-1; Hx, hemopexin*;* IQR, interquartile range; *Lrp1*, LDL-receptor related protein 1; *Lrp2*, LDL-receptor related protein 2; *Trf*, transferrin; Stx, Shiga toxin; WT, wild type.

Figure S11.

Supplementary Figure S11. Renal expression of DMT1, megalin and cubilin in WT, Hp$^{-/-}$ and Hx$^{-/-}$ mice with experimental HUS. Quantification and representative pictures of immunohistochemical (A) DMT1, (B) megalin and (C) cubilin staining on day 5 in renal sections of sham mice and mice

subjected to Stx (n = 8 per group). Bars = 100 µm. (A-B) Data are expressed as scatter dot plot with median ± IQR for n observations. *P < 0.05 vs. corresponding sham group, $^{§}P$ < 0.05 vs. WT Stx group (Mann-Whitney U-test). DMT1, divalent metal transporter 1; Hp, haptoglobin; Hx, hemopexin; IQR, interquartile range; Stx, Shiga toxin; ROI, region of interest; WT, wild type.

Figure S12.

Supplementary Figure S12. Oxidative stress in the kidney of WT, Hp$^{-/-}$ and Hx$^{-/-}$ mice with experimental HUS. (A) MDA levels on day 5 in kidneys of sham mice and mice subjected to Stx (n = 6 per group). Quantification of immunohistochemical (B) nitrotyrosine and (C) NOX-1 staining on day 5 in renal sections of sham mice and mice subjected to Stx (n = 8 per group). Bars = 100 µm. (A-C) Data are expressed as scatter dot plot with median ± IQR for n observations. *P < 0.05 vs. corresponding sham group, $^{\#}P$ < 0.05 vs. WT sham group, $^{§}P$ < 0.05 vs. WT Stx group (Mann-Whitney U-test). Hp, haptoglobin; Hx, hemopexin; IQR, interquartile range; MDA, malondialdehyde; NOX-1, NADPH oxidase 1; Stx, Shiga toxin; WT, wild type.

Supplementary References

Supplementary information is available on Kidney International's website.

References

1. Fakhouri F, Zuber J, Frémeaux-Bacchi V, Loirat C. Haemolytic uraemic syndrome. *Lancet*. Aug 12 2017;390(10095):681-696. doi:10.1016/s0140-6736(17)30062-4
2. Karmali MA. Infection by Shiga toxin-producing Escherichia coli: an overview. *Mol Biotechnol*. Feb 2004;26(2):117-22. doi:10.1385/mb:26:2:117
3. Riley LW, Remis RS, Helgerson SD, et al. Hemorrhagic colitis associated with a rare Escherichia coli serotype. *N Engl J Med*. Mar 24 1983;308(12):681-5. doi:10.1056/nejm198303243081203
4. Frank C, Werber D, Cramer JP, et al. Epidemic profile of Shiga-toxin-producing Escherichia coli O104:H4 outbreak in Germany. *N Engl J Med*. Nov 10 2011;365(19):1771-80. doi:10.1056/NEJMoa1106483
5. Proulx F, Seidman EG, Karpman D. Pathogenesis of Shiga toxin-associated hemolytic uremic syndrome. *Pediatr Res*. Aug 2001;50(2):163-71. doi:10.1203/00006450-200108000-00002
6. Mayer CL, Leibowitz CS, Kurosawa S, Stearns-Kurosawa DJ. Shiga toxins and the pathophysiology of hemolytic uremic syndrome in humans and animals. *Toxins (Basel)*. Nov 8 2012;4(11):1261-87. doi:10.3390/toxins4111261
7. Vinchi F, Costa da Silva M, Ingoglia G, et al. Hemopexin therapy reverts heme-induced proinflammatory phenotypic switching of macrophages in a mouse model of sickle cell disease. *Blood*. Jan 28 2016;127(4):473-86. doi:10.1182/blood-2015-08-663245
8. Larsen R, Gozzelino R, Jeney V, et al. A central role for free heme in the pathogenesis of severe sepsis. *Sci Transl Med*. Sep 29 2010;2(51):51ra71. doi:10.1126/scitranslmed.3001118
9. Merle NS, Grunenwald A, Rajaratnam H, et al. Intravascular hemolysis activates complement via cell-free heme and heme-loaded microvesicles. *JCI Insight*. Jun 21 2018;3(12)doi:10.1172/jci.insight.96910
10. Merle NS, Paule R, Leon J, et al. P-selectin drives complement attack on endothelium during intravascular hemolysis in TLR-4/heme-dependent manner. *Proc Natl Acad Sci U S A*. Mar 26 2019;116(13):6280-6285. doi:10.1073/pnas.1814797116
11. Dutra FF, Bozza MT. Heme on innate immunity and inflammation. *Front Pharmacol*. 2014;5:115. doi:10.3389/fphar.2014.00115
12. Wijnsma KL, Veissi ST, de Wijs S, et al. Heme as Possible Contributing Factor in the Evolvement of Shiga-Toxin Escherichia coli Induced Hemolytic-Uremic Syndrome. *Front Immunol*. 2020;11:547406. doi:10.3389/fimmu.2020.547406
13. Wang Y, Kinzie E, Berger FG, Lim SK, Baumann H. Haptoglobin, an inflammation-inducible plasma protein. *Redox Rep*. 2001;6(6):379-85. doi:10.1179/135100001101536580
14. Nielsen MJ, Moestrup SK. Receptor targeting of hemoglobin mediated by the haptoglobins: roles beyond heme scavenging. *Blood*. Jul 23 2009;114(4):764-71. doi:10.1182/blood-2009-01-198309
15. Kristiansen M, Graversen JH, Jacobsen C, et al. Identification of the haemoglobin scavenger receptor. *Nature*. Jan 11 2001;409(6817):198-201. doi:10.1038/35051594
16. Tolosano E, Hirsch E, Patrucco E, et al. Defective recovery and severe renal damage after acute hemolysis in hemopexin-deficient mice. *Blood*. Dec 1 1999;94(11):3906-14.
17. Gburek J, Verroust PJ, Willnow TE, et al. Megalin and cubilin are endocytic receptors involved in renal clearance of hemoglobin. *J Am Soc Nephrol*. Feb 2002;13(2):423-30.
18. Smith A, McCulloh RJ. Hemopexin and haptoglobin: allies against heme toxicity from hemoglobin not contenders. *Front Physiol*. 2015;6:187. doi:10.3389/fphys.2015.00187
19. Tolosano E, Cutufia MA, Hirsch E, Silengo L, Altruda F. Specific expression in brain and liver driven by the hemopexin promoter in transgenic mice. *Biochem Biophys Res Commun*. Jan 26 1996;218(3):694-703. doi:10.1006/bbrc.1996.0124
20. Paoli M, Anderson BF, Baker HM, Morgan WT, Smith A, Baker EN. Crystal structure of hemopexin reveals a novel high-affinity heme site formed between two beta-propeller domains. *Nat Struct Biol*. Oct 1999;6(10):926-31. doi:10.1038/13294
21. Hvidberg V, Maniecki MB, Jacobsen C, Højrup P, Møller HJ, Moestrup SK. Identification of the receptor scavenging hemopexin-heme complexes. *Blood*. Oct 1 2005;106(7):2572-9. doi:10.1182/blood-2005-03-1185
22. Ryter SW, Alam J, Choi AM. Heme oxygenase-1/carbon monoxide: from basic science to therapeutic applications. *Physiol Rev*. Apr 2006;86(2):583-650. doi:10.1152/physrev.00011.2005
23. Bitzan M, Bickford BB, Foster GH. Verotoxin (shiga toxin) sensitizes renal epithelial cells to increased heme toxicity: possible implications for the hemolytic uremic syndrome. *J Am Soc Nephrol*. Sep 2004;15(9):2334-43. doi:10.1097/01.Asn.0000138547.51867.43
24. Suttner DM, Dennery PA. Reversal of HO-1 related cytoprotection with increased expression is due to reactive iron. *Faseb j*. Oct 1999;13(13):1800-9. doi:10.1096/fasebj.13.13.1800

25. Maines MD. The heme oxygenase system: a regulator of second messenger gases. *Annu Rev Pharmacol Toxicol*. 1997;37:517-54. doi:10.1146/annurev.pharmtox.37.1.517
26. Epsztejn S, Glickstein H, Picard V, et al. H-ferritin subunit overexpression in erythroid cells reduces the oxidative stress response and induces multidrug resistance properties. *Blood*. Nov 15 1999;94(10):3593-603.
27. Lawson DM, Artymiuk PJ, Yewdall SJ, et al. Solving the structure of human H ferritin by genetically engineering intermolecular crystal contacts. *Nature*. Feb 7 1991;349(6309):541-4. doi:10.1038/349541a0
28. Hentze MW, Muckenthaler MU, Galy B, Camaschella C. Two to tango: regulation of Mammalian iron metabolism. *Cell*. Jul 9 2010;142(1):24-38. doi:10.1016/j.cell.2010.06.028
29. Lim SK, Kim H, Lim SK, et al. Increased susceptibility in Hp knockout mice during acute hemolysis. *Blood*. Sep 15 1998;92(6):1870-7.
30. Dennhardt S, Pirschel W, Wissuwa B, et al. Modeling Hemolytic-Uremic Syndrome: In-Depth Characterization of Distinct Murine Models Reflecting Different Features of Human Disease. *Front Immunol*. 2018;9:1459. doi:10.3389/fimmu.2018.01459
31. Sobbe IV, Krieg N, Dennhardt S, Coldewey SM. Involvement of NF-κB1 and the Non-Canonical NF-κB Signaling Pathway in the Pathogenesis of Acute Kidney Injury in Shiga-Toxin-2-Induced Hemolytic-Uremic Syndrome in Mice. *Shock*. May 18 2020;doi:10.1097/shk.0000000000001558
32. Pfaffl MW. A new mathematical model for relative quantification in real-time RT-PCR. *Nucleic Acids Res*. May 1 2001;29(9):e45. doi:10.1093/nar/29.9.e45
33. Rivero-Gutiérrez B, Anzola A, Martínez-Augustin O, de Medina FS. Stain-free detection as loading control alternative to Ponceau and housekeeping protein immunodetection in Western blotting. *Anal Biochem*. Dec 15 2014;467:1-3. doi:10.1016/j.ab.2014.08.027
34. Ofori-Acquah SF, Hazra R, Orikogbo OO, et al. Hemopexin deficiency promotes acute kidney injury in sickle cell disease. *Blood*. Mar 26 2020;135(13):1044-1048. doi:10.1182/blood.2019002653
35. Tolosano E, Fagoonee S, Hirsch E, et al. Enhanced splenomegaly and severe liver inflammation in haptoglobin/hemopexin double-null mice after acute hemolysis. *Blood*. Dec 1 2002;100(12):4201-8. doi:10.1182/blood-2002-04-1270
36. Ascenzi P, di Masi A, Fanali G, Fasano M. Heme-based catalytic properties of human serum albumin. *Cell Death Discov*. 2015;1:15025. doi:10.1038/cddiscovery.2015.25
37. Porubsky S, Federico G, Müthing J, et al. Direct acute tubular damage contributes to Shigatoxin-mediated kidney failure. *J Pathol*. Sep 2014;234(1):120-33. doi:10.1002/path.4388
38. Ozaki M, Kang Y, Tan YS, et al. Human mannose-binding lectin inhibitor prevents Shiga toxin-induced renal injury. *Kidney Int*. Oct 2016;90(4):774-82. doi:10.1016/j.kint.2016.05.011
39. Motto DG, Chauhan AK, Zhu G, et al. Shigatoxin triggers thrombotic thrombocytopenic purpura in genetically susceptible ADAMTS13-deficient mice. *J Clin Invest*. Oct 2005;115(10):2752-61. doi:10.1172/jci26007
40. Keepers TR, Psotka MA, Gross LK, Obrig TG. A murine model of HUS: Shiga toxin with lipopolysaccharide mimics the renal damage and physiologic response of human disease. *J Am Soc Nephrol*. Dec 2006;17(12):3404-14. doi:10.1681/asn.2006050419
41. Inward CD, Howie AJ, Fitzpatrick MM, Rafaat F, Milford DV, Taylor CM. Renal histopathology in fatal cases of diarrhoea-associated haemolytic uraemic syndrome. British Association for Paediatric Nephrology. *Pediatr Nephrol*. Oct 1997;11(5):556-9. doi:10.1007/s004670050337
42. Walters MD, Matthei IU, Kay R, Dillon MJ, Barratt TM. The polymorphonuclear leucocyte count in childhood haemolytic uraemic syndrome. *Pediatr Nephrol*. Apr 1989;3(2):130-4. doi:10.1007/bf00852893
43. Fernandez GC, Gomez SA, Ramos MV, et al. The functional state of neutrophils correlates with the severity of renal dysfunction in children with hemolytic uremic syndrome. *Pediatr Res*. Jan 2007;61(1):123-8. doi:10.1203/01.pdr.0000250037.47169.55
44. Yang H, Wang H, Levine YA, et al. Identification of CD163 as an antiinflammatory receptor for HMGB1-haptoglobin complexes. *JCI Insight*. 2016;1(7)doi:10.1172/jci.insight.85375
45. Moulouel B, Houamel D, Delaby C, et al. Hepcidin regulates intrarenal iron handling at the distal nephron. *Kidney Int*. Oct 2013;84(4):756-66. doi:10.1038/ki.2013.142
46. Fagoonee S, Gburek J, Hirsch E, et al. Plasma protein haptoglobin modulates renal iron loading. *Am J Pathol*. Apr 2005;166(4):973-83. doi:10.1016/s0002-9440(10)62319-x
47. Spiller F, Costa C, Souto FO, et al. Inhibition of neutrophil migration by hemopexin leads to increased mortality due to sepsis in mice. *Am J Respir Crit Care Med*. Apr 1 2011;183(7):922-31. doi:10.1164/rccm.201002-0223OC

48. Arredouani MS, Kasran A, Vanoirbeek JA, Berger FG, Baumann H, Ceuppens JL. Haptoglobin dampens endotoxin-induced inflammatory effects both in vitro and in vivo. *Immunology*. Feb 2005;114(2):263-71. doi:10.1111/j.1365-2567.2004.02071.x

49. Argyle JC, Hogg RJ, Pysher TJ, Silva FG, Siegler RL. A clinicopathological study of 24 children with hemolytic uremic syndrome. A report of the Southwest Pediatric Nephrology Study Group. *Pediatr Nephrol*. Jan 1990;4(1):52-8. doi:10.1007/bf00858440

50. Vogt BA, Shanley TP, Croatt A, Alam J, Johnson KJ, Nath KA. Glomerular inflammation induces resistance to tubular injury in the rat. A novel form of acquired, heme oxygenase-dependent resistance to renal injury. *J Clin Invest*. Nov 1 1996;98(9):2139-45. doi:10.1172/jci119020

51. Shimizu H, Takahashi T, Suzuki T, et al. Protective effect of heme oxygenase induction in ischemic acute renal failure. *Crit Care Med*. Mar 2000;28(3):809-17. doi:10.1097/00003246-200003000-00033

52. Nath KA, Balla G, Vercellotti GM, et al. Induction of heme oxygenase is a rapid, protective response in rhabdomyolysis in the rat. *J Clin Invest*. Jul 1992;90(1):267-70. doi:10.1172/jci115847

53. Theurl I, Hilgendorf I, Nairz M, et al. On-demand erythrocyte disposal and iron recycling requires transient macrophages in the liver. *Nat Med*. Aug 2016;22(8):945-51. doi:10.1038/nm.4146

54. Seixas E, Gozzelino R, Chora A, et al. Heme oxygenase-1 affords protection against noncerebral forms of severe malaria. *Proc Natl Acad Sci U S A*. Sep 15 2009;106(37):15837-42. doi:10.1073/pnas.0903419106

55. van Setten PA, van Hinsbergh VW, van der Velden TJ, et al. Effects of TNF alpha on verocytotoxin cytotoxicity in purified human glomerular microvascular endothelial cells. *Kidney Int*. Apr 1997;51(4):1245-56. doi:10.1038/ki.1997.170

56. Oh SK, Pavlotsky N, Tauber AI. Specific binding of haptoglobin to human neutrophils and its functional consequences. *J Leukoc Biol*. Feb 1990;47(2):142-8. doi:10.1002/jlb.47.2.142

57. Lill JK, Thiebes S, Pohl JM, et al. Tissue-resident macrophages mediate neutrophil recruitment and kidney injury in shiga toxin-induced hemolytic uremic syndrome. *Kidney Int*. Aug 2021;100(2):349-363. doi:10.1016/j.kint.2021.03.039

58. Lennon R, Singh A, Welsh GI, et al. Hemopexin induces nephrin-dependent reorganization of the actin cytoskeleton in podocytes. *J Am Soc Nephrol*. Nov 2008;19(11):2140-9. doi:10.1681/asn.2007080940

59. Bakker WW, Borghuis T, Harmsen MC, et al. Protease activity of plasma hemopexin. *Kidney Int*. Aug 2005;68(2):603-10. doi:10.1111/j.1523-1755.2005.00438.x

60. Cheung PK, Klok PA, Baller JF, Bakker WW. Induction of experimental proteinuria in vivo following infusion of human plasma hemopexin. *Kidney Int*. Apr 2000;57(4):1512-20. doi:10.1046/j.1523-1755.2000.00996.x

61. Zhou XJ, Vaziri ND, Pandian D, et al. Urinary concentrating defect in experimental hemochromatosis. *J Am Soc Nephrol*. Jan 1996;7(1):128-34.

62. Zhou XJ, Laszik Z, Wang XQ, Silva FG, Vaziri ND. Association of renal injury with increased oxygen free radical activity and altered nitric oxide metabolism in chronic experimental hemosiderosis. *Lab Invest*. Dec 2000;80(12):1905-14. doi:10.1038/labinvest.3780200

63. Kallianpur AR, Bradford Y, Mody RK, et al. Genetic Susceptibility to Postdiarrheal Hemolytic-Uremic Syndrome After Shiga Toxin-Producing Escherichia coli Infection: A Centers for Disease Control and Prevention FoodNet Study. *J Infect Dis*. Mar 5 2018;217(6):1000-1010. doi:10.1093/infdis/jix633

64. Nielsen R, Christensen EI, Birn H. Megalin and cubilin in proximal tubule protein reabsorption: from experimental models to human disease. *Kidney Int*. Jan 2016;89(1):58-67. doi:10.1016/j.kint.2015.11.007

65. Dixon SJ, Lemberg KM, Lamprecht MR, et al. Ferroptosis: an iron-dependent form of nonapoptotic cell death. *Cell*. May 25 2012;149(5):1060-72. doi:10.1016/j.cell.2012.03.042

66. NaveenKumar SK, SharathBabu BN, Hemshekhar M, Kemparaju K, Girish KS, Mugesh G. The Role of Reactive Oxygen Species and Ferroptosis in Heme-Mediated Activation of Human Platelets. *ACS Chem Biol*. Aug 17 2018;13(8):1996-2002. doi:10.1021/acschembio.8b00458

67. Ferraris V, Acquier A, Ferraris JR, Vallejo G, Paz C, Mendez CF. Oxidative stress status during the acute phase of haemolytic uraemic syndrome. *Nephrol Dial Transplant*. Mar 2011;26(3):858-64. doi:10.1093/ndt/gfq511

68. Monnens L, Molenaar J, Lambert PH, Proesmans W, van Munster P. The complement system in hemolytic-uremic syndrome in childhood. *Clin Nephrol*. Apr 1980;13(4):168-71.

69. Arvidsson I, Ståhl AL, Hedström MM, et al. Shiga toxin-induced complement-mediated hemolysis and release of complement-coated red blood cell-derived microvesicles in hemolytic uremic syndrome. *J Immunol*. Mar 1 2015;194(5):2309-18. doi:10.4049/jimmunol.1402470

70. Morigi M, Galbusera M, Gastoldi S, et al. Alternative pathway activation of complement by Shiga toxin promotes exuberant C3a formation that triggers microvascular thrombosis. *J Immunol*. Jul 1 2011;187(1):172-80. doi:10.4049/jimmunol.1100491
71. Ståhl AL, Sartz L, Karpman D. Complement activation on platelet-leukocyte complexes and microparticles in enterohemorrhagic Escherichia coli-induced hemolytic uremic syndrome. *Blood*. May 19 2011;117(20):5503-13. doi:10.1182/blood-2010-09-309161

Acknowledgements

We thank Jacqueline Fischer (Translational Septomics, Jena University Hospital, Jena, Germany) for technical assistance and Miguel Soares (Insitituto Gulbenkian de Ciência, Oeiras, Portugal) for providing us the breeding pairs of the knockout strains. We thank Michael Kiehntopf and Cora Richert from the Department of Clinical Chemistry and Laboratory Medicine, Jena University Hospital, for the measurement of plasma creatine, potassium and alanine aminotransferase. Mouse symbols were created with BioRender. The research leading to these results has received funding from the German Research Foundation (DFG, Research Unit FOR1738, award no. CO912/2-1 to SMC, award no. BA1601/8-2 to MB, award no. HE2993/12-2 to SHH) and the Federal Ministry of Education and Research (BMBF, ZIK Septomics Research Center, Translational Septomics, award no. 03Z22JN12 to SMC).

718 **Figure Legends**

719

720 **Figure 1. Clinical presentation of WT, Hp$^{-/-}$, and Hx$^{-/-}$ mice with experimental HUS.** (**a**) Kaplan-Meier
721 survival analysis of sham mice and mice subjected to Stx (WT sham: n = 9, WT Stx: n = 14, Hp$^{-/-}$ sham:
722 n = 8, Hp$^{-/-}$ Stx: n = 8, Hx$^{-/-}$ sham: n = 8, Hx$^{-/-}$ Stx: n = 8) in experimental HUS followed up for 7 days.
723 *P < 0.05 vs. corresponding sham group, $^{§}P$ < 0.05 vs. indicated Stx group (Log-rank Mantel-Cox test).
724 (**b-e**) Experimental HUS followed up for 5 days in sham mice and mice subjected to Stx (WT sham:
725 n = 19, WT Stx: n = 14, Hp$^{-/-}$ sham: n = 13, Hp$^{-/-}$ Stx: n = 13, Hx$^{-/-}$ sham: n = 12, Hx$^{-/-}$ Stx: n = 12).
726 (**b**) Evaluation of disease progression by HUS score (ranging from 1 = very active to 5 = dead) over 5
727 days. (**c**) Significant changes of HUS score on day 5 of sham mice and mice subjected to Stx.
728 (**d**) Progression of weight loss on day 1 to 5 in sham mice and mice subjected to Stx. (**e**) Significant
729 changes of weight loss on day 5 in sham mice and mice subjected to Stx. (**b-e**) Data are expressed as
730 (**b, d**) dot plot, (**c**) bar graph, (**e**) scatter dot plot with median ± IQR. *P < 0.05 vs. corresponding sham
731 group, $^{§}P$ < 0.05 vs. WT Stx group (Mann-Whitney *U*-test). Hp, haptoglobin; Hx, hemopexin; IQR,
732 interquartile range; Stx, Shiga toxin; WT, wild type.

733

734 **Figure 2. Heme and Hb scavengers in WT, Hp$^{-/-}$, and Hx$^{-/-}$ mice with experimental HUS.** (**a**) mRNA
735 expression of *Hx* on day 5 in livers of sham mice and mice subjected to Stx (n = 6 per group, except:
736 n = 5 for Hp$^{-/-}$ Stx). (**b**) Plasma Hx levels on day 5 of sham mice and mice subjected to Stx (n = 12 per
737 group). Determination of plasma (**c**) α1M and (**d**) albumin on day 5 in sham mice and mice subjected to
738 Stx (n = 12 per group). (**e**) mRNA expression of *Hp* on day 5 in livers of sham mice and mice subjected
739 to Stx (n = 6 per group). (**f**) Plasma Hp levels on day 5 of sham mice and mice subjected to Stx (n = 12
740 per group). (**a-e**) Data are expressed as scatter dot plot with median ± IQR for n observations. *P < 0.05
741 vs. corresponding sham group, $^{#}P$ < 0.05 vs. WT sham group, $^{§}P$ < 0.05 vs. WT Stx group
742 (Mann-Whitney *U*-test). α1M, alpha-1-microglobulin; *Hp*/Hp, haptoglobin; *Hx*/Hx, hemopexin; IQR,
743 interquartile range; Stx, Shiga toxin; WT, wild type.

744

745 **Figure 3. Kidney injury and renal stress burden in WT, Hp$^{-/-}$, and Hx$^{-/-}$ mice with experimental**
746 **HUS.** Determination of plasma (**a**) urea and (**b**) NGAL on day 5 in sham mice and mice subjected to Stx
747 (n = 12 per group). Quantification of (**c**) PAS reaction on day 5 in renal sections of sham mice and mice
748 subjected to Stx (n = 8 per group). Quantification and representative pictures of immunohistochemical

(**d**) KIM-1 staining on day 5 in renal sections of sham mice and mice subjected to Stx (n = 8 per group). Quantification of immunohistochemical (**e**) CD31 and (**f**) CC-3 staining on day 5 in renal sections of sham mice and mice subjected to Stx (n = 8 per group). (**g**) Protein expression of HO-1 on day 5 in kidneys of sham mice and mice subjected to Stx. Samples from 6 animals per group were pooled to equal protein amounts for this representative blot (n = 6 per group). Individual blots (1 animal/group) are shown in supplementary Figure S1A. (**h**) Quantification and representative pictures of immunohistochemical GP1b staining on day 5 in renal sections of sham mice and mice subjected to Stx (n = 8 per group). Bars = 100 µm. Data are expressed as (**a-f, h**) scatter dot plot, (**g**) bar graph with median ± IQR for n observations. **P* < 0.05 vs. corresponding sham group, $^{\#}$*P* < 0.05 vs. WT sham group (Mann-Whitney *U*-test). CC-3, cleaved caspase-3; GP1b; glycoprotein 1b; Hp, haptoglobin; HO-1, heme oxygenase-1; Hx, hemopexin; IQR, interquartile range; KIM-1, kidney injury molecule-1; NGAL, neutrophil gelatinase-associated lipocalin; PAS, periodic acid Schiff; Stx, Shiga toxin, WT, wild type.

Figure 4. Hemolysis in WT, Hp$^{-/-}$, and Hx$^{-/-}$ mice with experimental HUS. Determination of (**a**) hemolysis and (**b**) plasma bilirubin on day 5 in sham mice and mice subjected to Stx (hemolysis: WT sham: n = 10, WT Stx n = 10, Hp$^{-/-}$ sham n = 8, Hp$^{-/-}$ n = 7, Hx$^{-/-}$ sham n = 8, Hx$^{-/-}$ Stx n = 9; bilirubin: n = 12 per group). (**c**) mRNA expression of *Hmox1* on day 5 in the liver of sham mice and mice subjected to Stx (n = 6 per group). Protein expression of HO-1 on day 5 in the liver of (**d**) WT, (**e**) Hp$^{-/-}$, and (**f**) Hx$^{-/-}$ sham mice and mice subjected to Stx (n = 5 per group). Protein expression of Fth1 on day 5 in the liver of (**g**) WT, (**h**) Hp$^{-/-}$, and (**i**) Hx$^{-/-}$ sham mice and mice subjected to Stx (n = 5 per group). Protein expression of CD163 on day 5 in the liver of (**j**) WT, (**k**) Hp$^{-/-}$, and (**l**) Hx$^{-/-}$ sham mice and mice subjected to Stx (n = 5 per group). (**a-l**) Data are expressed as scatter dot plot with median ± IQR for n observations. **P* < 0.05 vs. corresponding sham group. Fth1, ferritin heavy chain; Hp, haptoglobin; *Hmox1*/HO-1; heme oxygenase-1; Hx, hemopexin; Stx, Shiga toxin; WT, wild type.

Figure 5. Immune response in WT, Hp$^{-/-}$, and Hx$^{-/-}$ mice with experimental HUS. Quantification and representative pictures of immunohistochemical (**a**) F4-80, (**b**) Ly6G, and (**c**) C3c staining on day 5 in renal sections of sham mice and mice subjected to Stx (n = 8 per group). Bars = 100 µm. (**a-c**) Data are expressed as scatter dot plot with median ± IQR for n observations. **P* < 0.05 vs. corresponding sham group, $^{\#}$*P* < 0.05 vs. WT sham group, §*P* < 0.05 vs. WT Stx group (Mann-Whitney *U*-test). Hp,

779 haptoglobin; Hx, hemopexin; IQR, interquartile range; Ly6G, lymphocyte antigen 6 complex, locus G;
780 Stx, Shiga toxin; WT, wild type.
781
782 **Figure 6. Effect of Hp treatment on kidney injury and inflammation in WT mice with experimental**
783 **HUS.** (**a**) Application regime for low dose Hp treatment of sham mice and mice subjected to Stx.
784 (**b**) Determination of plasma NGAL on day 5 in sham mice and mice subjected to Stx, which were treated
785 with Hp or vehicle (n = 6 per treatment group). Quantification of (**c**) PAS reaction, immunohistochemical
786 (**d**) KIM-1, (**e**) CC-3, (**f**) F4-80, (**g**) C3c, (**h**) GP1b and (**i**) Ly6G staining on day 5 in renal sections of
787 sham mice and mice subjected to Stx, which were treated with Hp or vehicle (sham + vehicle,
788 sham + Hp: n = 4 per group; Stx + vehicle, Stx + Hp: n = 6 per group; GP1b: Stx + Hp: n = 5 per group).
789 (**c-h**) Data are expressed as scatter dot plot with median ± IQR for n observations. **P* < 0.05 vs.
790 corresponding sham group (Mann-Whitney *U*-test). CC-3, cleaved caspase-3; GP1b; glycoprotein 1b;
791 Hp, haptoglobin; i.p., intraperitoneal; IQR, interquartile range; KIM-1, kidney injury molecule-1; Ly6G,
792 lymphocyte antigen 6 complex, locus G; NGAL, neutrophil gelatinase-associated lipocalin; PAS, periodic
793 acid Schiff, s.c., subcutaneous; Stx, Shiga toxin, WT, wild type.
794
795 **Figure 7. Renal iron homeostasis in WT, Hp$^{-/-}$, and Hx$^{-/-}$ mice with experimental HUS.**
796 (**a**) Quantification and representative pictures of iron staining on day 5 in renal sections of sham mice
797 and mice subjected to Stx (n = 8 per group). (**b**) Protein expression of Fth1 on day 5 in kidneys of sham
798 mice and mice subjected to Stx. Samples from 6 animals per group were pooled to equal protein
799 amounts for this representative blot (n = 6 per group). Individual blots (1 animal/group) are shown in
800 supplementary Figure S1B. (**c**) Plasma hepcidin levels on day 5 of sham mice and mice subjected to
801 Stx (n = 6 per group). Quantification and representative pictures of immunohistochemical (**d**) ferroportin
802 staining on day 5 in renal sections of sham mice and mice subjected to Stx (n = 8 per group).
803 Bars = 100 µm. Data are expressed as (**a, c-d**) scatter dot plot, (**b**) bar graph with median ± IQR for n
804 observations. **P* < 0.05 vs. corresponding sham group, $^{\#}P$ < 0.05 vs. WT sham group, $^{\S}P$ < 0.05 vs. WT
805 Stx group (Mann-Whitney *U*-test). Fth1, ferritin heavy chain; Hp, haptoglobin; Hx, hemopexin; IQR,
806 interquartile range; Stx, Shiga toxin; ROI, region of interest; WT, wild type.
807
808

Figure 1

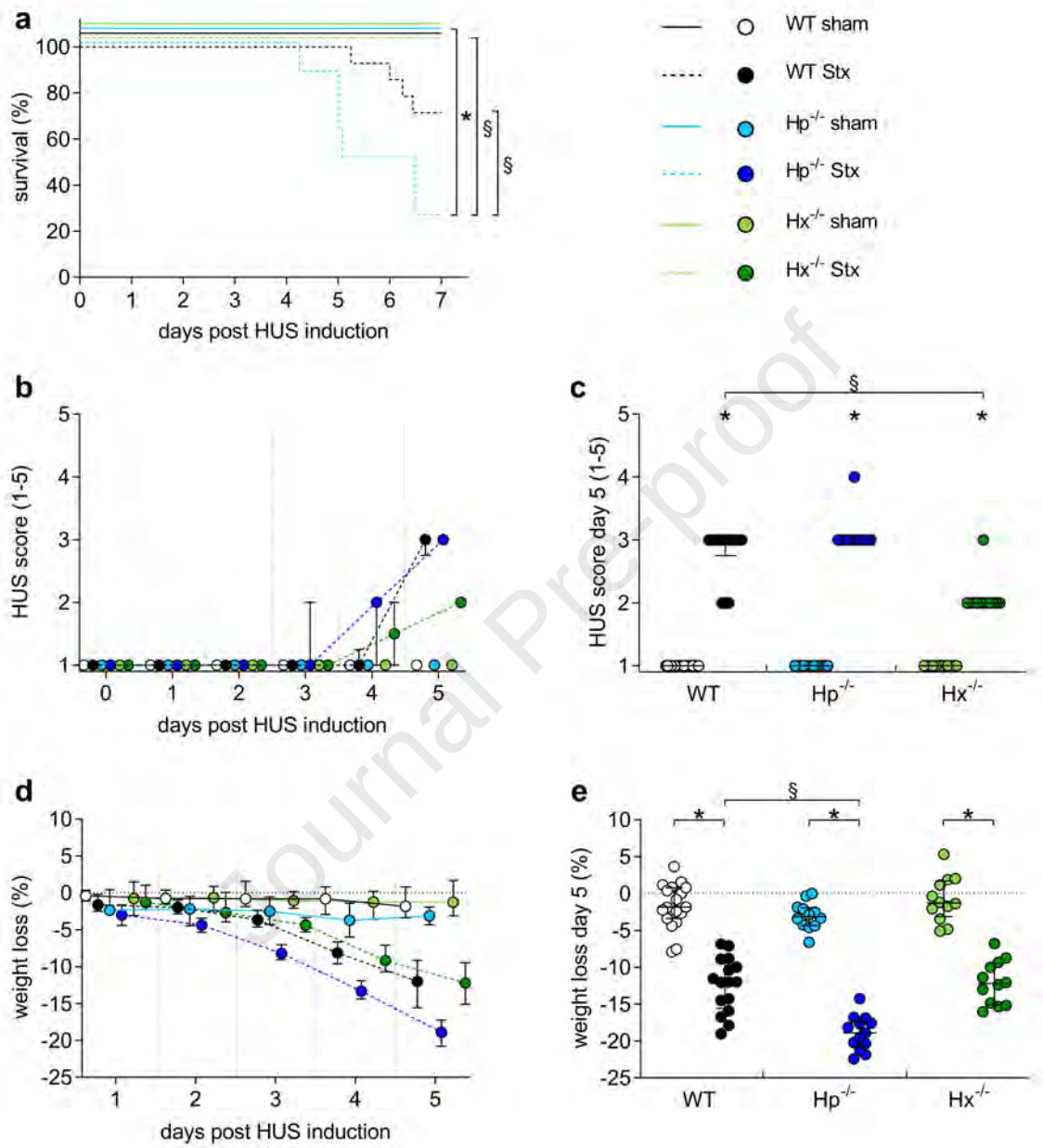

Figure 2

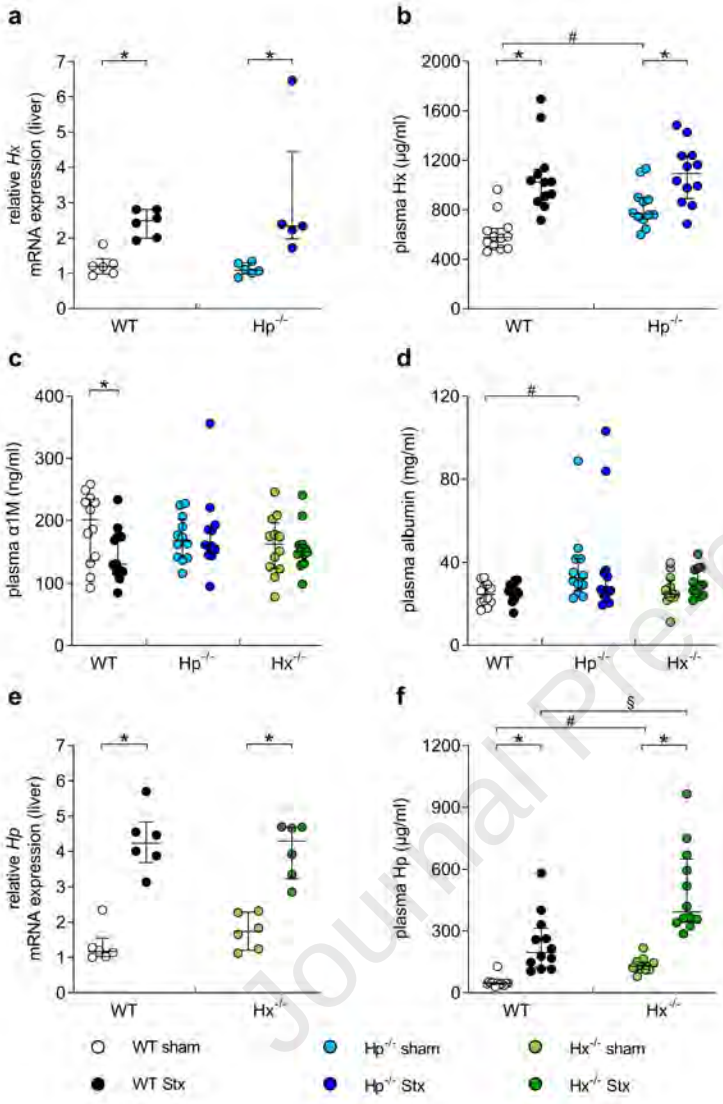

Figure 3

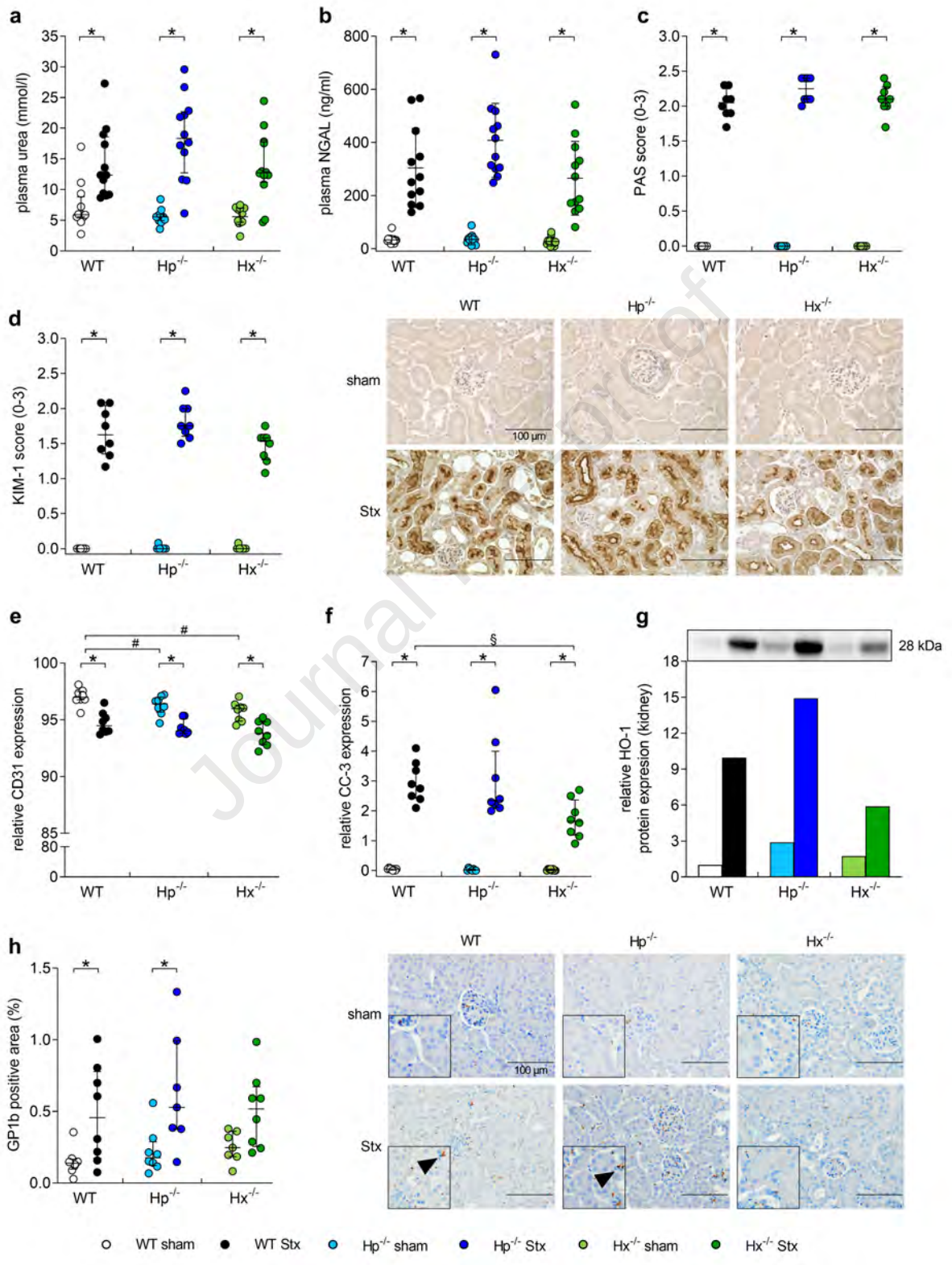

Figure 4

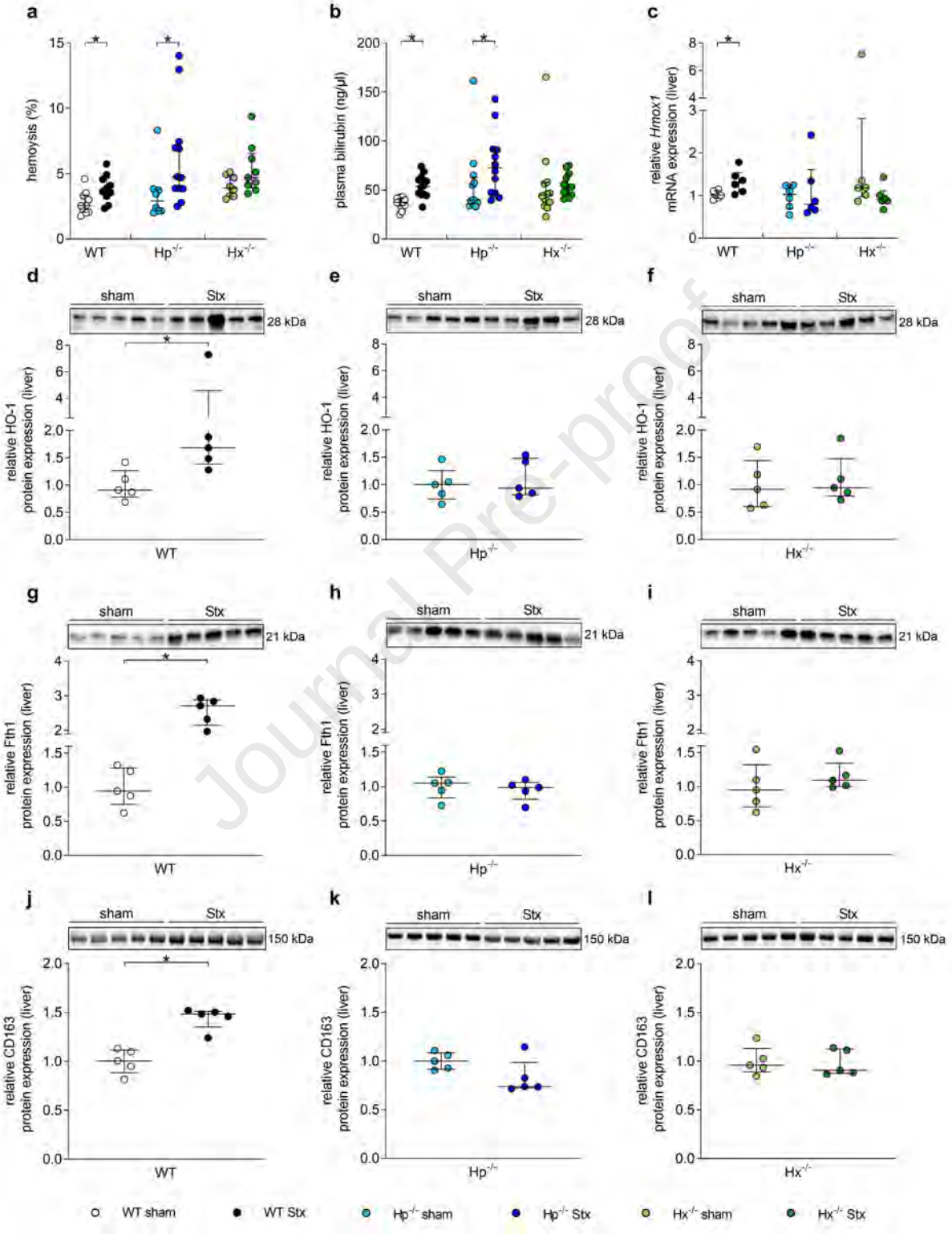

Figure 5

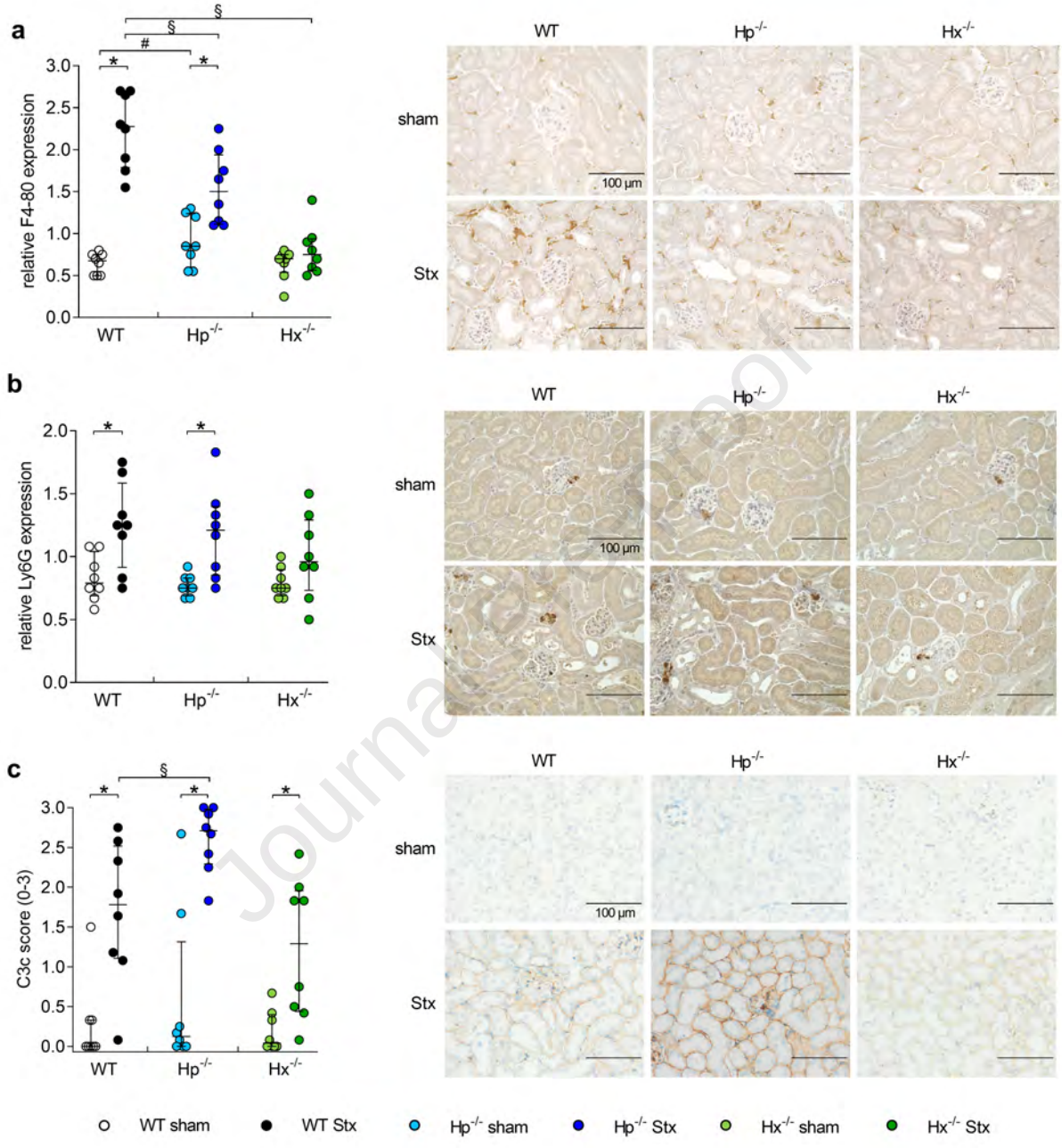

Figure 6

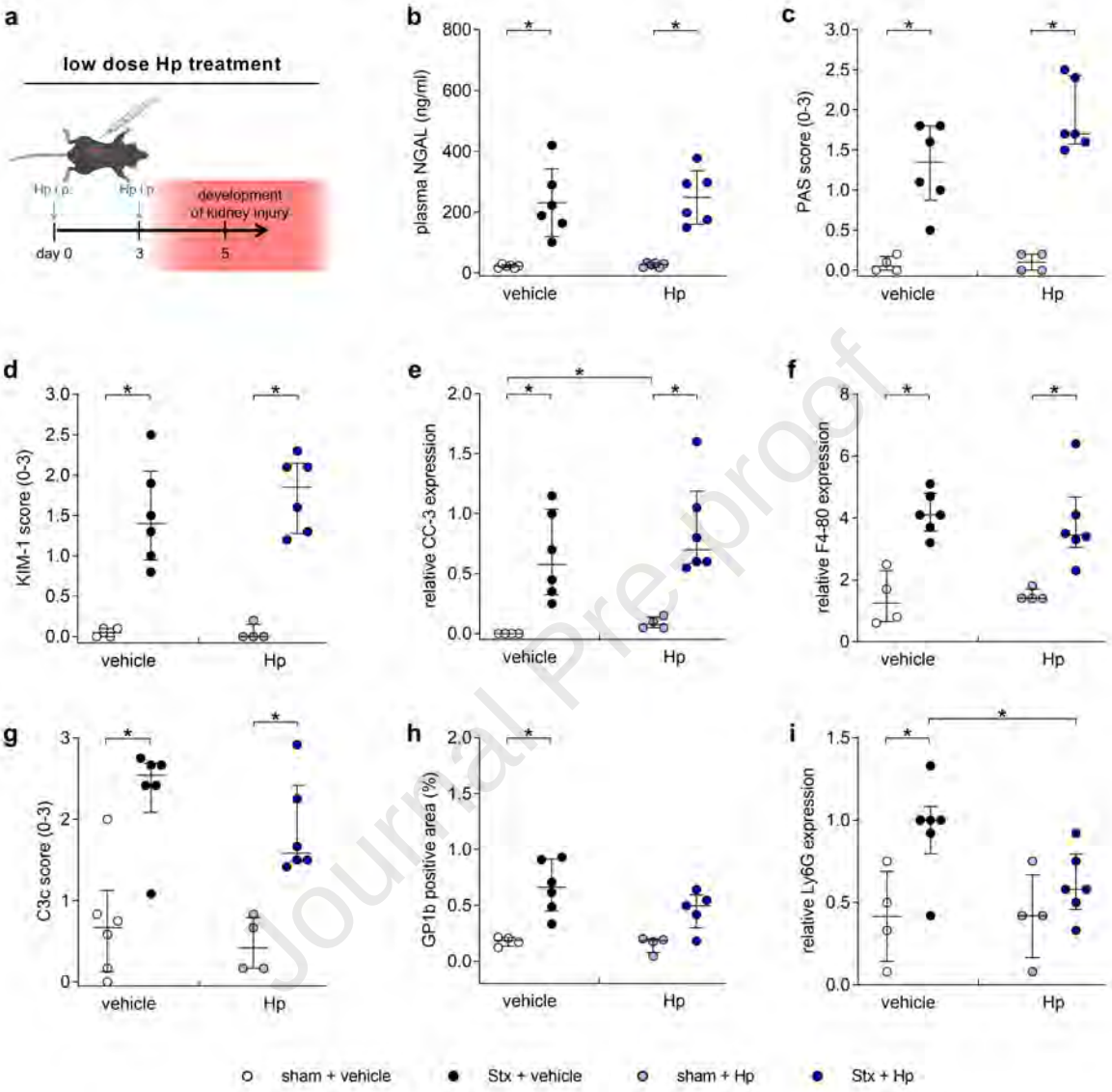

Figure 7